This is the accepted version of the article submitted to Key Engineering Materials, which has been published in final form at 10.4028/www.scientific.net/KEM.484.172.

Effect of NH_3 atmosphere on preparation of Al_2O_3–AlN composite film by laser CVD

Yu You[1,a], Akihiko Ito[1,b], Rong Tu[1,c] and Takashi Goto[1,d]

[1]Institute for Materials Research, Tohoku University, Sendai 980-8577, Japan

[a]youyu@imr.tohoku.ac.jp, [b]itonium@imr.tohoku.ac.jp,
[c]turong@imr.tohoku.ac.jp, [d]goto@imr.tohoku.ac.jp

Keywords: Al_2O_3, AlN, composite film, laser CVD

Abstract. Al_2O_3–AlN composite film was first prepared by laser chemical vapor deposition (laser CVD) using aluminum acetylacetonate ($Al(acac)_3$) and ammonia (NH_3) as source materials. The effects of NH_3 on the crystal phase, composition and microstructure were investigated. The crystal phase changed from α-Al_2O_3 to AlN gradually with increasing the mole ratio of NH_3 to Ar. Al_2O_3-AlN composite film was obtained at NH_3/Ar ratio ranged from 0.09 to 0.16 (T_{dep} = 862–887 K), and AlN granular grains were embedded in between α-Al_2O_3 polyhedral grains.

Introduction

Al_2O_3 thin film has been an important material used as protective coating for cutting tool inserts because of its high hardness and oxidation resistance [1–3]. However, its relatively low thermal conductivity of 25 W m^{-1} K^{-1} cannot realize efficient heat dissipation, and thus inhabits its applications to fields where high thermal conduction is needed, such as heat exchanger and heat pipe [4]. On the other hand, Aluminum nitride (AlN) has a high thermal conductivity of 140–180 W m^{-1} K^{-1}. The Al_2O_3–AlN composite of both bulk and film materials have been studied as an effort to enhance the thermal conductivity of Al_2O_3 [5–8]. Since AlN also has excellent corrosion resistance to molten salts, the successful preparation of Al_2O_3–AlN composite can expand the application of Al_2O_3 coating for, such as graphite crucible [9]. However, γ-AlON had been found to be formed during the sintering process of Al_2O_3-AlN bulk material. Although AlON itself is a good optical ceramics, the formation of AlON in Al_2O_3-AlN system would limit the improvement of system thermal conductivity because the thermal conductivity of AlON is only 10 W m^{-1} K^{-1} [5]. As for Al_2O_3–AlN composite film, usually, Al_2O_3 and AlN were prepared separately and the sample surface was often contaminated [10,11], resulting in a weak bonding strength between Al_2O_3 and AlN grains. Therefore, another process to prepare high continuity Al_2O_3–AlN composite should be developed.

$Al(acac)_3$ was widely used as the aluminum source material for preparation of Al_2O_3 film because of its non-toxicity, low cost, good stability at room temperature and high volatility at elevated temperature [12-14]. The high-speed, low-temperature preparation of Al_2O_3 and AlN films with using $Al(acac)_3$ by a newly-developed laser chemical vapor deposition (laser CVD) had been reported [15, 16]. In the present study, by examining the effect of NH_3, we report on the preparation of Al_2O_3–AlN composite film on YSZ substrate and investigate the effects of deposition conditions on the crystal phase, composition and microstructure of Al_2O_3–AlN composite films.

Experimental procedure

A vertical, cold-wall type CVD chamber equipped with an InGaAlAs diode laser (wavelength: 808 nm) was used to prepare Al_2O_3–AlN composite film [15]. YSZ plates (10 mm × 10 mm × 1 mm) were used as substrates. The laser beam was introduced into the chamber through a quartz-glass window and was slightly expanded by lenses to irradiate the whole substrate. The laser was operated in continuous mode at power (P_L) 140 W. A thermocouple was inserted into a slot engraved from the back with 0.5 mm distance to the surface of substrate to measure the deposition temperature (T_{dep}). $Al(acac)_3$ (99%) precursor was evaporated by electrical heating and its vapor was transported into the chamber using Ar gas (99.99%). The $Al(acac)_3$ precursor vaporization temperature (T_{Al}) was set at

This is the accepted version of the article submitted to Key Engineering Materials, which has been published in final form at 10.4028/www.scientific.net/KEM.484.172.

433 K and the flow rate of Ar (FR_{Ar}) carrier gas was fixed at 1.65×10^{-6} m^3 s^{-1}. NH_3 gas (99.9995%) was introduced separately into the chamber through a double-tube nozzle. The flow rate of NH_3 (FR_{NH_3}) gas was controlled in a range of 0–1.65×10^{-6} m^3 s^{-1}. The ratio between NH_3 and Ar flow rates ($R_{NH_3} = FR_{NH_3}/FR_{Ar}$) was changed from 0 to 1. The total pressure (P_{tot}) in the CVD chamber was fixed at 0.2 kPa. The feed pipes and the nozzle were heated at 523 K to prevent condensation of the precursor vapor.

The crystal phases of the composite films were examined by θ–2θ X-ray diffraction with Cu Kα radiation (XRD; Rigaku, RAD-2C) and the chemical bonding was analyzed by X-ray photoelectron spectroscopy with Al Kα radiation (XPS; Shimadzu Kratos, Axis-Ultra DLD). The morphology of composite films was characterized using a scanning electron microscope (SEM; Hitachi, S-3100H). The composition was measured by an electron probe micro analyzer (EPMA; JEOL, JXA-8530F).

Results and discussion

Figure 1 shows the effect of the R_{NH3} on the XRD patterns of Al_2O_3–AlN composite films prepared at T_{Al} = 433 K, P_{tot} = 0.2 kPa and P_L = 140 W. The peaks of α-Al_2O_3 crystal phase were identified at R_{NH3} = 0 (Fig. 1 (a)), implying α-Al_2O_3 was formed by pyrolysis of $Al(acac)_3$ [14, 17]. At R_{NH3} = 0.09, wurtzite AlN was identified in a low intensity, and other XRD peaks were identified as α- and also γ-Al_2O_3 (Fig. 1 (b)). The peak intensity of α-Al_2O_3 was attenuated with increasing R_{NH3} to 0.16; meanwhile, the peak intensity of AlN became stronger (Fig. 1 (c)). At R_{NH3} = 0.25, single-phase AlN film was obtained (Fig. 1 (d)).

Figure 2 shows the binding energy spectra of Al 2*p* for the Al_2O_3–AlN composite films prepared at T_{Al} = 433 K, P_{tot} = 0.2 kPa, P_L = 140 W and R_{NH3} = 0 to 1. As a binding energy reference, the C 1*s* peak from contamination carbon was set at 284.6 eV [18]. The Al 2*p* spectra were deconvoluted into two components with binding energy of 74.0 ± 0.2 eV and 74.4 ± 0.2 eV. The component with binding energy of 74.0±0.2 eV is assigned to aluminum bound to nitrogen (AlN), and the other component is assigned to aluminum bound to oxygen (Al_2O_3) [18, 19]. At R_{NH3} = 0, the Al 2*p*-O component was well coincide with the Al 2*p* scan peak, while the Al 2*p*-N component was in approximately background intensity. The intensity of Al 2*p*-N component increased with increasing R_{NH3}, while the intensity of Al 2*p*-O component decreased with increasing R_{NH3}, implying a high NH_3 concentration was favorable for the formation of AlN crystal phase. At R_{NH3} = 1, Al 2*p*-N component was well coincide with the Al 2*p* scan peak. The Al 2*p*-O component was simultaneously identified in a low intensity, implying small amount Al_2O_3 was always appear on the surface of deposited composite films. This can be due to a thin oxide layer formed on the AlN film surface.

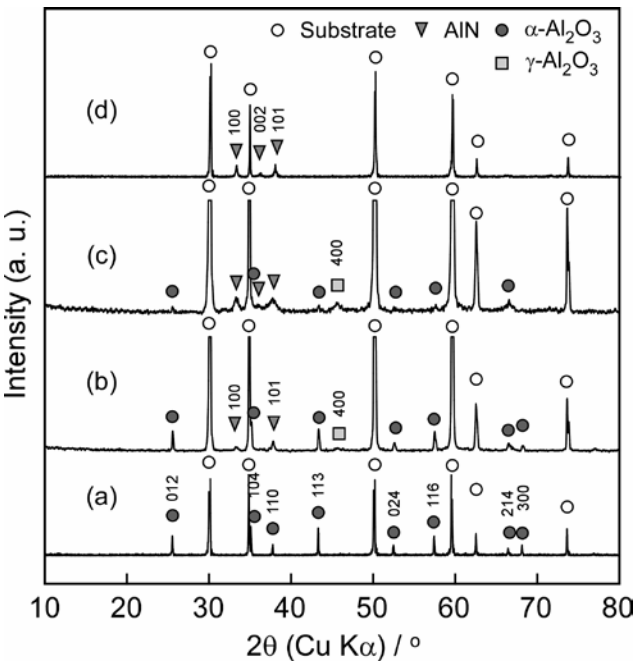

Fig. 1. XRD patterns of Al_2O_3–AlN composite films prepared at T_{Al} = 433 K, P_{tot} = 0.2 kPa and P_L = 140 W: (a) R_{NH3} = 0 and T_{dep} = 893 K, (b) R_{NH3} = 0.09 and T_{dep} = 862 K, (c) R_{NH3} = 0.16 and T_{dep} = 887 K, (d) R_{NH3} = 0.25 and T_{dep} = 873 K.

Figure 3 shows the binding energy spectra of N 1s for the Al_2O_3-AlN composite films prepared at T_{Al} = 433 K, P_{tot} = 0.2 kPa, P_L = 140 W, and R_{NH3} = 0 to 1. The spectra were dominated by two photoelectron peaks located at 397.1 ± 0.2 eV and 400.2 ± 0.1 eV. The lower binding energy peak can be

This is the accepted version of the article submitted to Key Engineering Materials, which has been published in final form at 10.4028/www.scientific.net/KEM.484.172.

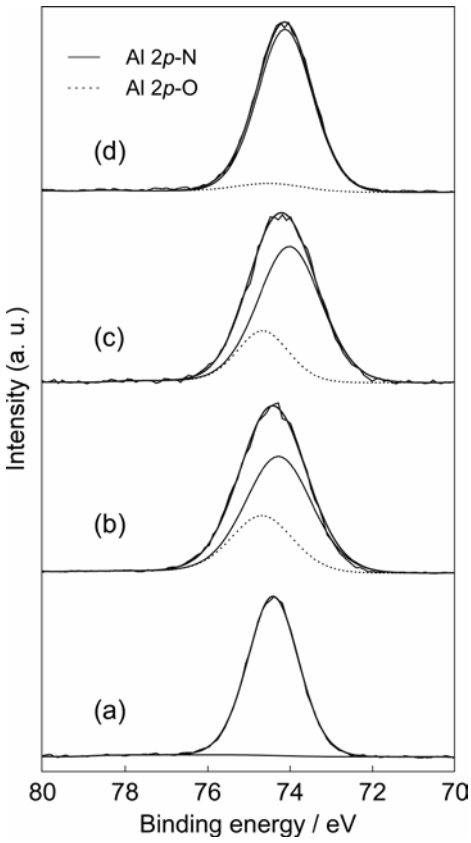

Fig. 2. Al 2*p* XPS spectra of Al_2O_3–AlN composite films prepared at T_{Al} = 433 K, P_{tot} = 0.2 kPa, P_L = 140 W and (a) R_{NH3} = 0 and T_{dep} = 893 K, (b) R_{NH3} = 0.09 and T_{dep} = 862 K, (c) R_{NH3} = 0.16 and T_{dep} = 887 K, (d) R_{NH3} = 1.0 and T_{dep} = 843 K.

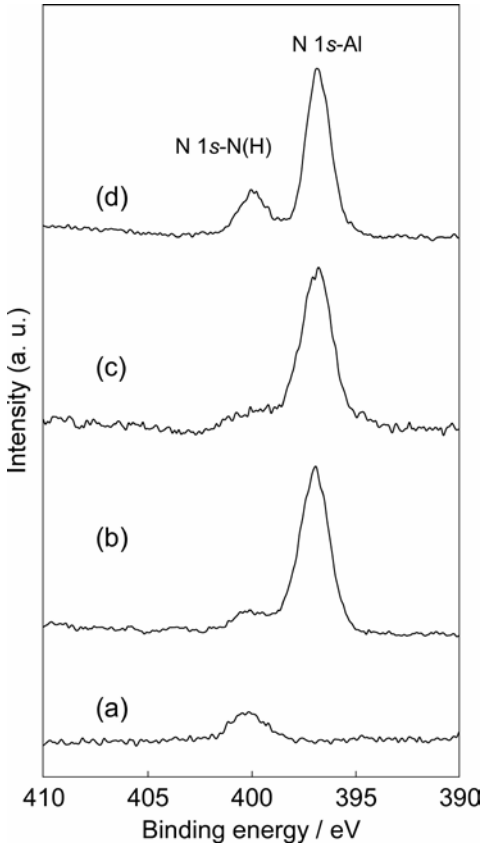

Fig. 3. N 1*s* XPS spectrum of Al_2O_3–AlN composite films prepared at T_{Al} = 433 K, P_{tot} = 0.2 kPa, P_L = 140 W and (a) R_{NH3} = 0 and T_{dep} = 893 K, (b) R_{NH3} = 0.09 and T_{dep} = 862 K, (c) R_{NH3} = 0.16 and T_{dep} = 887 K, (d) R_{NH3} = 1.0 and T_{dep} = 843 K.

attributed to nitrogen bound to aluminum, since its binding energy is in well agreement with previously published values for AlN films [18, 20]. The peaks with higher binding energy could be assigned to nitrogen molecular adsorbed on the sample surface, because this peak was always identified even in the case of without introducing NH_3 gas (R_{NH3} = 0).

Figure 4 shows the SEM images of Al_2O_3–AlN composite films prepared at T_{Al} = 433 K, P_{tot} = 0.2 kPa, P_L = 140 W, and R_{NH3} = 0 to 0.25. At R_{NH3} = 0, the morphology corresponding to Al_2O_3 grains was characterized by polyhedral shape (Fig. 4(a)). With increasing R_{NH3} to 0.09, the observed microstructure consisted of two kinds of grains. One is polyhedral grains grown in a manner of continuous matrix, which may be corresponding to α-Al_2O_3 as compared with Fig. 4(a). The other one is granular grains being dispersed uniformly to the interstice of polyhedral grains (Fig. 4(b)). EPMA analysis revealed that the N element is highly contained in the granular grains, implying the granular grains were mainly composed of AlN crystal. With increasing R_{NH3} to 0.16 and 0.25, the morphology changed completely from polyhedral grains to granular grains

The deposition temperature is an influential parameter for crystal growth in CVD process. α-Al_2O_3 film was commonly prepared at temperatures around 1323 K [1, 3]. In contrast, AlN film was prepared at 873–1623 K, and its morphology changed from powder to pebble to facet with increasing deposition temperature [21, 22]. A relatively low crystallization temperature of Al_2O_3–AlN composite film in the present study can be associated with the laser irradiation, which accelerated the decomposition of precursors and promoted the grain growth of deposits. The difference in microstructure of Al_2O_3 and AlN grains suggested that the surface diffusion of O species were more

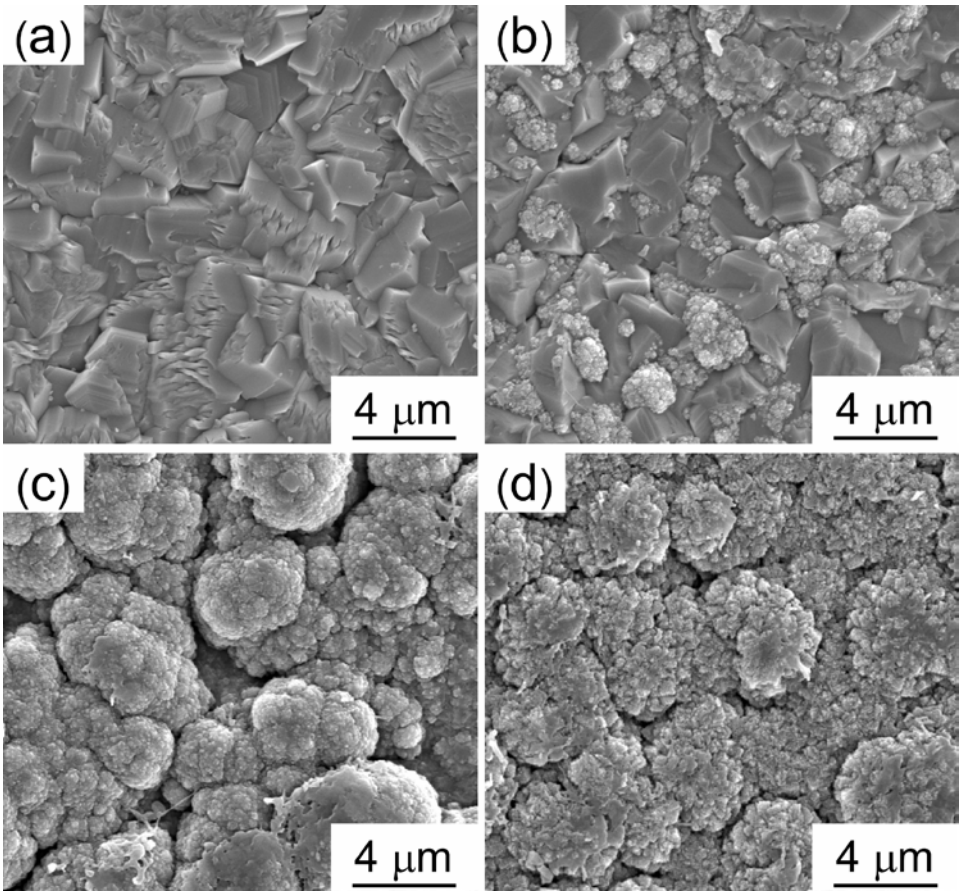

Fig. 4. Surface SEM images of Al_2O_3–AlN composite films prepared at T_{Al} = 433 K, P_{tot} = 0.2 kPa, P_L = 140 W: (a) R_{NH3} = 0 and T_{dep} = 893 K, (b) R_{NH3} = 0.09 and T_{dep} = 862 K, (c) R_{NH3} = 0.16 and T_{dep} = 887 K, (d) R_{NH3} = 0.25 and T_{dep} = 873 K.

significant than that of N species, causing a prominent grain growth of Al_2O_3 grains while a localized nucleation of AlN grains.

Summary

We firstly prepared Al_2O_3–AlN composite films by laser CVD using $Al(acac)_3$ and NH_3 gas as source materials, and investigated the effect of R_{NH3} on the crystal phases and microstructure. The crystal phase changed from Al_2O_3 to AlN gradually with increasing R_{NH3}. The coexistence of AlN and α-Al_2O_3 crystals phase was confirmed at R_{NH3} ranged from 0.09 to 0.16 (T_{dep} = 862–887 K). The surface morphology was characterized by irregular polyhedral grains at R_{NH3} = 0, and changed to granular structure with crystal phase changed from Al_2O_3 to AlN. The Al_2O_3-AlN composite film prepared at R_{NH3} = 0.09 was characterized by an obviously continuous matrix of α-Al_2O_3 polyhedral grains with granular AlN grains being embedded uniformly.

Acknowledgments

This study was supported in part by the Global COE Program of Materials Integration, Tohoku University, and in part by the Rare Metal Substitute Materials Development Project of the New Energy and Industrial Technology Development Organization (NEDO). This study was also supported in part by the Japan Society for the Promotion of Science, Grant-in-Aid for Young Scientists (B), No. 22760550, and by the Ministry of Education, Culture, Sports, Science and Technology, Grant-in-Aid for Scientific Research (A), No. 22246082.

References

[1] B. Lux, C. Colombier, H. Altena and K. Stjernberg: Thin Solid Films Vol. 138 (1986), p. 49

[2] S. Ruppi and A. Larsson: Thin Solid Films Vol. 388 (2001), p. 50

[3] R. Connelly, A.K. Pattanaik, V.K. Sarin: Int. J. Refract. Met. Hard Mater Vol. 23 (2005), p. 317

[4] H. Yang, W. Luan and S.-T. Tu: Mater. Trans. Vol. 47 (2006), p. 1649

[5] F.Y.C. Boey, X.L. Song, Z.Y. Gu and A. Tok: J. Mater. Process. Technol. Vol. 89–90 (1999), p. 478

[6] F.Y.C. Boey, L. Sun, X. Song and K.A. Khor: J. Mater. Sci.: Mater. Electron. Vol. 10 (1999), p. 455

[7] L.H. Cao, K.A. Khor, L. Fu and F. Boey: J. Mater. Process. Technol. Vol. 89–90 (1999), p. 392

[8] Y.W. Kim, H.C. Park, Y.B. Lee, K.D. Oh and R. Stevens: J. Eur. Ceram. Soc. Vol. 21 (2001), p. 2383

[9] T. Watanabe, M. Kondo, T. Nagasaka, A. Sagara: Proceedings of the 7th General Scientific Assembly of the Asia Plasma and Fusion Association in 2009 (APFA2009) and Asia-Pacific Plasma Theory Conference in 2009 (APPTC2009), Japan, (2010), p. 342

[10] I. Kimura, N. Hotta, M. Ishii and M. Tanaka: J. Mater. Sci. Vol. 26 (1991), p. 258

[11] Q. Zheng and R. Reddy: Metall. Mater. Trans. B Vol. 34 (2003), p. 793

[12] A. Devi, S.A. Shivashankar and A.G. Samuelson: J. de Phys. IV Vol. 12 (2002), p. 139

[13] C. Pflitsch, A. Muhsin, U. Bergmann and B. Atakan: Surf. Coat. Technol. Vol. 201 (2006), p. 73

[14] T. Maruyama and S. Arai: Appl. Phys. Lett. Vol. 60 (1992), p. 322

[15] Y. You, A. Ito, R. Tu and T. Goto: Appl. Surf. Sci. Vol. 256 (2010), p. 3906

[16] A. Ito, H. Kadokura, T. Kimura and T. Goto: J. Alloys Compd. Vol. 489 (2010), p. 469

[17] M.P. Singh and S.A. Shivashankar: Surf. Coat. Technol. Vol. 161 (2002), p. 135

[18] R. Leland, B. Ronald, M. Erik, A. Gregory and S. Gina: Surf. Interface Anal. Vol. 40 (2008), p. 1254

[19] F. Martin and P. Muralt: Appl. Phys. Lett. Vol. 88 (2006), p. 242506

[20] H. Liu, D.C. Bertolet and J.W. Rogers Jr: Surf. Sci. Vol. 320 (1994), p. 145

[21] A.J. Noreika and D.W. Ing: J. Appl. Phys. Vol. 39 (1968), p. 5578

[22] T. Goto, J. Tsuneyoshi, K. Kaya and T. Hirai: J. Mater. Sci. Vol. 27 (1992), p. 247